DYNAMICS OF CHIRAL QUASIPARTICLES IN A NOISY ENVIRONMENT: TOWARDS QUANTUM CONTROL

Marco Berritta, Elisabetta Paladino, Antonio D'Arrigo and Giuseppe Falci
MATIS-INFM-CNR Catania
DMFCI-Universitá degli studi di Catania
Italy
marco@femto.dmfci.unict.it

Abstract

We study the dynamics of a chiral particle obeyng Weyl equation and coupled to a bosonic environment. The model describes the dynamics of quasiparticles in graphene sheets, in the presence of noisy controls, simulating external electromagnetic quantum fields. Wavepackets show Spin Separation and Zitterbewegung at mesoscopic scales, which are suppressed in a peculiar way by quantum fluctuations of the environment. Here we present some exact result.

Key words

Nanotechnologies, Quantum control, Qauntum information.

1 Introduction

The recent discovery that individual graphene sheets can be isolated [14] has stimulated a renewed interest in carbon-based materials. Indeed graphene has distinguished mechanical and electrical properties, as the large mobility, which makes it attractive for applications in nanoelectronics. Graphene is two-dimensional carbon arranged in a honeycomb lattice. Due to the symmetries of the lattice, the (nonrelativistic) "effective mass" Hamiltonian for Quasi-Particles (QP) close to the symmetry (Dirac) points of the Brillouin zone [2] is formally identical to the relativistic Hamiltonian for Quantum Electrodynamics in 2 dimensions. In a single valley QP's have a gapless linear energy-momentum dispersion and their dynamics is described by the quantum mechanical Weyl Hamiltonian for massles Dirac fermions. For a graphene sheet lying in the $x-y$ plane, and subject to a uniform electric field in the y direction $\mathbf{E} = E(t)\,\mathbf{e}_y$ the Hamiltonian reads

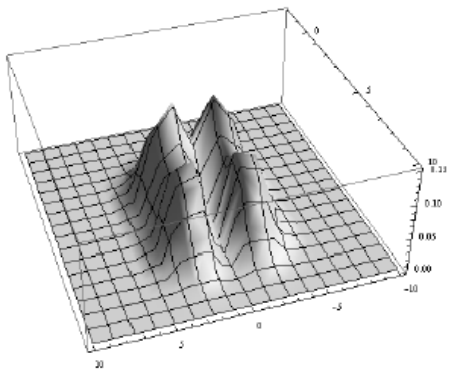

Figure 1. Spatial profile of the total density $\rho^{\sigma}(r,t)$ The ρ^{ZB} component (consistent of the of diagonal part of $\rho^{\sigma}(r,t)$)produces a modulation of the total density in the region between two maximum of spin separation.

$$\mathcal{H}_W \;=\; v\,\hat{\mathbf{p}}\cdot\boldsymbol{\sigma}+eE(t)\,\hat{y} \;=\; v\left[\hat{\mathbf{p}}-\frac{e}{c}\,A(t)\,\mathbf{e}_y\right]\cdot\boldsymbol{\sigma} \quad (1)$$

where $\hat{y}$ is the operator of the y-component of the QP and $E(t) = \frac{1}{c}\frac{\partial A}{\partial t}$, $A = A(t)e_y$ being the vector pontential in absence of magnetic field. Here $\boldsymbol{\sigma}$ is a pseudospin operator, the eigenstates of σ_z corresponding to the QP tight-binding wavefunctions on each sublattice of the honeycomb structure (the physical spin is conserved and we ignore it), and v is the Fermi velocity, playing the role of the speed of light in the relativistic version. QP's are chiral due to spin-momentum coupling: the hamiltonian expressed in terms of the vector potential shows that quantum control of the pseudospin dynamics is possible via electric fields coupling with a QP coordinate. Therefore phototransport could be in principle modulated using quantum control protocols tipical of the quantum optics realm [4]. This roadmap naturally extends to microscopic degrees of freedom one of the most fascinating experimental breakthroughs of the recent past, namely the observation of coherent pseudospin dynamics in nanodevices based on superconductors [20] and semiconductors.

1.1 Spin separation and Zitterbewegung

The dynamics of isolated wave-packets of Weyl QP's shows many distinct features. Contrary to massive non relativistic particles, wave-packets of Weyl QP's from a single helicity branch experience a very weak breadth, due to the linear dispersion implying that each component travels at the same velocity v. On the other hand new phenomena appear for superposition of states from different branches. Since the direction of the velocity depends on the helicity such a wave-packet will separate in two opposite moving components (SS). Interference between them gives rise to ZB. This features are usually discussed in the Heisenberg picture [8] in which the equation of motion for the speed operator are:

$$\hat{v} = i[\hat{r}, H] = v\hat{\vec{\sigma}} \tag{2}$$

and for instance ZB is associated to a part $\mathbf{r}_{ZB}(t)$ of the position operator oscillating in time with angular frequency $\Omega(\mathbf{k}) = 2v|\mathbf{k}|$, the energy splitting of two states $|\mathbf{k}\,\sigma_{\mathbf{k}}\rangle$ with the same $\mathbf{k}$ and opposite helicity. Instead we use the Schrödinger picture, which is conveniently generalized to an open system. For the representation we use the *chiral basis* of the eigenstates of Eq.(1). The density matrix in the laboratory frame is given by

$$\zeta^L(t) = \sum_{\mathbf{k}\sigma\mathbf{k}'\sigma'} |\mathbf{k}\sigma_{\mathbf{k}}\rangle\langle\mathbf{k}'\sigma'_{\mathbf{k}'}|\, \zeta^L_{\mathbf{k}\sigma\mathbf{k}'\sigma'}(0)\, \mathrm{e}^{-iv(|\mathbf{k}|\sigma - |\mathbf{k}'|\sigma')t}$$

In order to calculate averages of interest we introduce the operators $P_\sigma = \sum_{\mathbf{k}\sigma} |\mathbf{k}\sigma_{\mathbf{k}}\rangle\langle\mathbf{k}\sigma_{\mathbf{k}}|$ projecting on a well defined component ($\sigma = \pm 1$) of the helicity $\sigma_{\mathbf{k}}$. Any operator $\hat{A}$ can be decomposed in "diagonal" parts $P_\sigma \hat{A} P_\sigma$ and "off diagonal" parts $P_\sigma \hat{A} P_{-\sigma}$ these latter describing interference. In particular letting $\hat{A} = \delta(\hat{\mathbf{r}}(t) - \mathbf{r})$ the average of the diagonal parts represent the probability densities $\varrho^\sigma(\mathbf{r}, t)$ of two spin-separated wave-packets, whereas the average of the interference terms yields $\varrho^{ZB}(\mathbf{r}, t)$, which is a spatial modulation between the two wave-packets above, oscillating with time. The associated centroid is the average of the oscillating part of the position operator

$$\langle \mathbf{r}_{ZB}(t)\rangle = \sum_{\mathbf{k}\sigma} \mathbf{A}_{\sigma,-\sigma}(\mathbf{k})\, \zeta^L_{\mathbf{k}-\sigma\,\mathbf{k}\sigma}(t)$$

Here $\sum_{\mathbf{k}} \to \int \frac{d\mathbf{k}}{2\pi}$ in the continuum limit (not always specified hereafter). The connection in k-space associated to the chiral basis appears $\mathbf{A}_{\sigma\sigma'}(\mathbf{k}) = i\langle\sigma_{\mathbf{k}}|\nabla_{\mathbf{k}}\sigma'_{\mathbf{k}}\rangle = \sigma\sigma'\,\mathbf{t}_{\mathbf{k}}/(2|\mathbf{k}|)$, where the unitary vector $\mathbf{t}_{\mathbf{k}}$ is such that $\{\mathbf{k}/|\mathbf{k}|, \mathbf{t}_{\mathbf{k}}, \mathbf{z}\}$ is a left-handed reference frame for the momentum space. Notice that the density matrix enters with elements diagonal in $\mathbf{k}$ and off diagonal in the pseudospin index σ.

2 Model.

The control of coherent dynamics opens ports to noise. In discussing the effect of the environment we recall that for a massive particle with ohmic damping [10] the wave-packet breadth grows only logarithmically on time, reflecting decoherence due to the environment measuring the particle position $\mathbf{r}$, while for finite temperatures diffusive behavior is found in the long time limit. We address the problem of noise by coupling Weyl QP's to an environment. To this end we supplement the Weyl hamiltonian with a part describing a set of quantum harmonic oscillators coupled linearly to the coordinate operator $\hat{y}$ of the QP, as in the Caldeira-Leggett model [1] [21]

$$\delta\mathcal{H} = -\hat{y}\sum_\alpha C_\alpha x_\alpha + \sum_\alpha \big(\frac{p_\alpha^2}{2m_\alpha} + \frac{m_\alpha\omega_\alpha^2}{2}\big)x_\alpha^2 + \hat{y}^2 \sum_\alpha \frac{C_\alpha^2}{2m_\alpha\omega_\alpha^2} \tag{3}$$

The state of the system described by this hamiltonian could be described by density matrix $W(t)$; We are interested only on the dynamics of quasiparticle. To this end we consider the Reduced Density Matrix (RDM) obteined tracing over the environment degree of freedom the total density matrix: $\hat{\zeta}^L(t) = \mathrm{Tr}_\alpha[W(t)]$ The relevant information on the environment is provided by the spectral density associated to X, given by $J_X(\omega) = \pi\sum_\alpha \frac{c_\alpha^2}{2m_\alpha\omega_\alpha}\delta(\omega - \omega_\alpha)$[21].

2.1 Dynamics in the QP-supported frame

In order to study the dynamics we first rescale the environment coordinates and momenta $y'_\alpha \to c_\alpha y_\alpha/m_\alpha\omega_\alpha^2$ and $p'_\alpha \to m_\alpha\omega_\alpha^2 p_\alpha/c_\alpha$. Then we perform on the resulting Hamiltonian $\mathcal{H}'$ a (polaron) transformation, represented by the unitary operator $U = \exp\big(-i\hat{y}\sum_\alpha \hat{p}_\alpha\big)$ which shifts the positions to y_α, now referred to the QP position. The effective Hamiltonian in this QP-supported frame, reads

$$\tilde{\mathcal{H}}(\hat{\mathbf{p}}) = U\,\mathcal{H}'\,U^\dagger = v\,\mathbf{p}\cdot\vec{\sigma} - \sigma_y\, v\sum_\alpha p_\alpha + \sum_\alpha \Big(\frac{p_\alpha^2}{2\mu_\alpha} + \frac{1}{2}\mu_\alpha\omega_\alpha^2\, y_\alpha^2\Big) \tag{4}$$

Therefore the coupling of the QP position $\mathbf{r}$ with the environmental $\hat{X}$ in Eq.(3) is gauged away in favor of a spin-boson like coupling of the pseudo-spin with environmental momenta. The effects of the transformation are fully defined by specifying the new spectral density

$$J_P(\omega) = \pi\sum_\alpha \frac{v^2}{2\mu_\alpha\omega_\alpha}\delta(\omega - \omega_\alpha) = \frac{v^2}{\omega^2}\, J_X(\omega) \tag{5}$$

Notice that the operator $\hat{\mathbf{p}}$, which is still the conjugate of $\hat{\mathbf{r}}$, is physically the total momentum of the system

and it is conserved. Therefore the dynamics is determined by the set of Hamiltonians $\mathcal{H}_{\mathbf{K}} = \tilde{\mathcal{H}}(\mathbf{K})$ depending parametrically on the eigenvalue $\mathbf{K}$ of $\mathbf{p}$. Each $\tilde{\mathcal{H}}_K$ acts on a spin-boson system only, and the problem is mapped in a spin-boson model, with *conditional* dynamics.

The evolution operator determined by the Hamiltonian (4) is given by $\mathcal{U}(t) = \sum_{\mathbf{K}} |\mathbf{K}\rangle\langle\mathbf{K}| \otimes \mathrm{e}^{-i\mathcal{H}_{\mathbf{K}}t}$ and allows to express the simplified dynamics of the full density matrix $\mathcal{W}(t) = U_T\, W(t)\, U_T^\dagger$ in the QP-supported frame. In view of the simplifications brought in by the conditional dynamics it is convenient to eliminate the microscopic degrees of freedom of the *modified* environment, labeled by $\tilde{\alpha}$, to obtain

$$\hat{\zeta}(t) = \mathrm{Tr}_{\tilde{\alpha}}[\mathcal{W}(t)] = \sum_{\mathbf{K}\sigma} |\mathbf{K}\sigma_{\mathbf{K}}\rangle\, \zeta^{(\mathbf{K},\mathbf{K}')}_{\sigma\sigma'}(t)\, \langle \mathbf{K}'\sigma'_{\mathbf{K}'}| \tag{6}$$

This RDM describes the *dressed* QP (polaron). It can be decomposed in a set of 2×2 operators $\zeta^{(\mathbf{K},\mathbf{K}')}$, each acting in a sector $(\mathbf{K},\mathbf{K}')$, and evolving independently. They are structurally reminiscent to the RDM of the spin-boson model, however the parametric dependence on $(\mathbf{K},\mathbf{K}')$ has non trivial features: for $\mathbf{K} \neq \mathbf{K}'$ the exact dynamics of $\zeta^{(\mathbf{K},\mathbf{K}')}$ is deformed [6], and it is not trace preserving.

Since the unitary transformation to the QP-supported frame preserves both the QP coordinate $\hat{\mathbf{r}}$ and the pseudo-spin, averages as the spin resolved densities $\varrho^{\sigma}(\mathbf{r},t)$ and $\varrho^{ZB}(\mathbf{r},t)$ can be calculated directly in the QP-supported frame. In particular we will evaluate

$$\begin{aligned}\varrho^{\sigma}(\mathbf{r},t) &= \textstyle\sum_{\mathbf{K}\mathbf{K}'} \mathrm{Tr}[\,|\mathbf{K}\rangle\langle\mathbf{K}'|\, \zeta^{(\mathbf{K}',\mathbf{K})}_{\sigma\sigma}(t)\, \delta(\hat{\mathbf{r}}-\mathbf{r})] \\ &= \textstyle\sum_{\mathbf{K}\mathbf{K}'} \mathrm{e}^{i(\mathbf{k}-\mathbf{k}')\cdot\mathbf{r}}\, \langle\, \sigma_{\mathbf{K}}|\sigma_{\mathbf{K}'}\rangle\, \zeta^{(\mathbf{K}',\mathbf{K})}_{\sigma\sigma}(t)\end{aligned} \tag{7}$$

$$\langle \mathbf{r}_{ZB}(t)\rangle = -\sum_{\mathbf{K}} \frac{\mathbf{t}_{\mathbf{K}}}{|\mathbf{K}|}\, \Re[\zeta^{(\mathbf{K},\mathbf{K})}_{+-}(t)] \tag{8}$$

In order to proceed we define sectors labeled by $(\mathbf{K},\mathbf{K}')$ and projected operators, for instance $\hat{\mathcal{W}}^{(\mathbf{K},\mathbf{K}')} = \langle\, \mathbf{K}\,|\hat{\mathcal{W}}\,|\mathbf{K}'\,\rangle$. Momentum conservation ensures that they evolve independently, undergoing a deformed dynamics

$$\hat{\mathcal{W}}^{(\mathbf{K},\mathbf{K}')}(t) = \mathrm{e}^{-i\mathcal{H}_{\mathbf{K}}t}\, \hat{\mathcal{W}}^{(\mathbf{K},\mathbf{K}')}(0)\, \mathrm{e}^{-i\mathcal{H}_{\mathbf{K}'}t}$$

2.2 Master equation.

Tracing out the environment one obtains the reduced operators $\hat{\zeta}^{(\mathbf{K},\mathbf{K}')}$ of the pseudo-spin Liouville space, appearing in Eq.(6). They solve an exact equation which can be written in a deformed interaction picture [6] as

$$\begin{aligned}&\tilde{\zeta}^{(\kappa\kappa')}(t+\Delta t) - \tilde{\zeta}^{(\kappa\kappa')}(t) \;= \\ &-\int_t^{t+\Delta t} dt' \int_t^{t'} dt''\; \mathrm{Tr}_{\tilde{\alpha}}\Big\{\big[\tilde{\mathcal{H}}_1(t'),\big[\tilde{\mathcal{H}}_1(t''),\tilde{\mathcal{W}}^{(\kappa\kappa')}(t'')\big]'\big]'\Big\}\end{aligned}$$

where Δt is a coarse graining time. Here $\tilde{\mathcal{H}}_1(t)$ ($\tilde{\mathcal{H}}'_1(t)$) is the QP-environment coupling of Eq.(4) in the interaction picture relative to the parameter $\mathbf{K}$ ($\mathbf{K}'$). Primed commutator, reflecting deformation of the dynamics, are defined as

$$[\tilde{\mathcal{H}}_1(t),\tilde{\mathcal{X}}]' = \tilde{\mathcal{H}}_1(t)\,\tilde{\mathcal{X}} - \tilde{\mathcal{X}}\,\tilde{\mathcal{H}}'_1(t) \tag{9}$$

At this stage an approximate closed equation for $\tilde{\zeta}^{(\kappa\kappa')}(t)$ can be obtained by first assuming factorized initial $\tilde{\mathcal{W}}^{(\kappa\kappa')}(0) = \tilde{\zeta}^{(\kappa\kappa')} \otimes w_{eq}$, where w_{eq} is the equilibrium density matrix of the environment, and then following the same lines leading to the Bloch-Redfield equation [4], which govern the dynamics in the sector $\mathbf{K} = \mathbf{K}'$.

Deformation of the dynamics implies that, besides the splitting of the helicity bands $\approx 2v|\mathbf{Q}|$, where $\mathbf{Q} = (\mathbf{K}+\mathbf{K}')/2$, a new energy scale enters the problem, related to $\mathbf{q} = \mathbf{K}-\mathbf{K}'$. For a wave-packet with a dispersion $\sim\Delta$ in in momentum space, the variable q may have values ranging from Δ to zero, therefore the associated energy scale may vanish. As a consequence there will always be sectors with non-secular deformed dynamics. This structure, becomes transparent for noise with white power spectrum $J_P(\omega)\coth(\beta\omega/2) \to 2\Gamma$. In this limit the problem has an exact solution, which is very useful to capture the essential consequences of the deformed dynamics. In this case the exact master equation in the Schrödinger picture for white noise becomes

$$\begin{aligned}\partial_t\, \zeta^{(\kappa\kappa')}(t) &= \mathcal{L}(\mathbf{Q},\mathbf{q})\;\cdot\hat{\zeta}^{(\kappa\kappa')}(t) \\ \mathcal{L}(\mathbf{Q},\mathbf{q})\,\hat{\zeta} &= -iv\big[\mathbf{Q}\cdot\vec{\sigma},\hat{\zeta}\big] - i\tfrac{v}{2}\big[\mathbf{q}\cdot\vec{\sigma},\hat{\zeta}\big]_+ \\ &\quad -\tfrac{\Gamma}{2}\,[\hat{\zeta} - \sigma_y\,\hat{\zeta}(t)\,\sigma_y]\end{aligned} \tag{10}$$

Notice here the presence of the anticommutator term containing $\mathbf{q}$. This term disappears for operators in diagonal sectors and Eq.(10) reduces to a standard Lindblad equation for a two-state atom with Bohr splitting $2v|\mathbf{Q}|$.

2.3 One dimensional wavepacket

We perform our calculation of dynamics of wave packets only in the case of one dimensional wave packets. They are, of the form:

$$g(\vec{k}) = \frac{A}{(2\pi\sigma_{kx}^2)^{1/4}} e^{\frac{-(k_x-k_x0)^2}{4\sigma_{kx}^2}} \tag{11}$$

In order to understand motion of a one-dimensional wave-packet in an arbitrary direction $\mathbf{n}$, we now specify to this case the exact Master Equation for white noise, Eq.(10). A convenient matrix form is obtained using the decomposition $\zeta^{(\kappa\kappa')}(t) = \frac{1}{2}\sum_{i=0}^{4} R_i(t)\,\sigma_i$, where $\{\sigma_i\} = \{I,\sigma_{\mathbf{n}},\sigma_{\mathbf{t}},\sigma_{\mathbf{z}}\}$ is a basis of the pseudo-

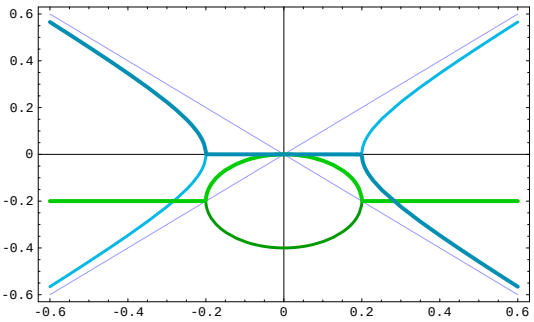

Figure 2. Schematic plot of the behavior of the eigenvalues $z_{0,1}$ for SS ($z_{2,3}$ for ZB) as given by Eq.(15) as a function of vq (vQ). Imaginary parts (blue) vanish in the overdamped regime $2vq < \Gamma$ ($4vQ < \Gamma$) wherea in the opposite limit they behave as $\sim \pm ivq$ ($\sim \pm ivQ$). In this limit real parts (green) are given by $(\Gamma/2)$ whereas in the overdamped limit, $\Re z \sim 0, \Gamma$, the zero value being associated to the Zeno effect.

spin Liouville space. For each sector the master equation reads $\dot{\mathbf{R}} = \mathcal{L}\,\mathbf{R}$ where

$$\mathcal{L} \equiv \begin{pmatrix} 0 & -iv\,q & 0 & 0 \\ -iv\,q_n & -\Gamma\,c^2 & \Gamma\,sc & 0 \\ 0 & \Gamma\,sc & -\Gamma\,s^2 & -2vQ \\ 0 & 0 & 2vQ & -\Gamma \end{pmatrix} \tag{12}$$

Notice that $R_0 = \mathrm{Tr}[\zeta^{(\mathbf{KK'})}]$ and $R_1 = \mathrm{Tr}[\zeta^{(\mathbf{KK'})}\sigma_{\mathbf{n}}]$ enter the spin separated densities, whereas R_2 and R_3 determine ϱ_{ZB}. We concentrate on the explicit calculation of the dynamics of one dimensional wave packet ($Q_t, q_t = 0$). In this case it is readily verified that for longitudinal noise ($\phi_{\mathbf{n}} = \pi/2$) the result agrees with the exact solution of sec. 3.1. Indeed noise does not enter the components R_0 and R_1: the two imaginary eigenvalues $\pm ivq$ of $\mathcal{L}$ lead to SS as for the isolated QP. The other two eigenvalues, given by $-\Gamma \pm 2ivQ$ yield damped ZB oscillations at the band splitting frequency, decaying at a rate Γ, which agrees with the proper limit of Eq.(14).

Instead for generic $\mathbf{n}$ all four eigenvalues have a non vanishing real part. This indicates that both SS and ZB have components $\hat{\zeta}^{(\mathbf{K},\mathbf{K'})}$ which are damped or even overdamped.

3 Results

3.1 Exact solution for longitudinal noise

If we set initially $K_x = 0$ the dynamics in each sector (K, K') involves the Hamiltonians of the form $\mathcal{H}_K = \mathcal{H}_{K\mathbf{e}_y}$. The helicity coincides with σ_y and it is conserved, since $[\mathcal{H}_K, \sigma_y] = 0$. Therefore eigenstates of the helicity are unaffected by longitudinal noise. Dynamics in each sector is given by

$$\zeta^{(KK')}_{\sigma\sigma'}(t) = \langle\,\sigma_y\,|\mathrm{Tr}_{\tilde{\alpha}}\left[\mathrm{e}^{-i\mathcal{H}_K t}\,\mathcal{W}^{(KK')}(0)\,\mathrm{e}^{i\mathcal{H}_{K'}t}\right]|\sigma'_y\,\rangle$$

Since it acts on its eigenstates the spin operator σ_y contained in each Hamiltonian can be replaced by a number, $\mathcal{H}_K\,|\sigma_y\,\rangle = (ivK\sigma + \mathcal{H}_\sigma)\,|\sigma_y\,\rangle$, where $\mathcal{H}_\sigma$ is the Hamiltonian (4) for $\mathbf{K} = 0$ and for $\sigma_x \to \sigma = \pm 1$. Using the cyclic property of the partial trace we obtain

$$\zeta^{(KK')}_{\sigma\sigma'}(t) = \mathrm{e}^{-i(K\sigma - K'\sigma')vt}\cdot \mathrm{Tr}_{\tilde{\alpha}}\left[\mathcal{W}^{(KK')}(0)\,\mathrm{e}^{i\mathcal{H}_{\sigma'}t}\mathrm{e}^{-i\mathcal{H}_\sigma t}\right] \tag{13}$$

We see that for diagonal elements the effect of the environment cancels, expressing helicity conservation. As a consequence spin resolved probability densities $\rho_\sigma(\mathbf{r}, t)$ evolve as in absence of the environment, fully displaying spin separation.

Instead off diagonal elements are affected by the presence of the environment. Assuming factorized initial conditions the partial trace for $\sigma' = -\sigma$ can be written as

$$\mathrm{Tr}_{\tilde{\alpha}}\left[\,\cdot\,\right] = \zeta^{(KK')}_{\sigma\,-\sigma}(0)\;\mathrm{e}^{-D(t)}$$

where $D(t)$ is a decay factor describing pure dephasing. Therefore longitudinal noise determines a suppression of interference effects in a superpositions of spin states and of ZB oscillations. For an oscillator environment one finds explicitly

$$D(t) = \int_0^\infty \frac{d\omega}{\pi}\,J_P(\omega)\,\coth\frac{\beta\omega}{2}\,\frac{1-\cos\omega t}{\omega^2} \tag{14}$$

for an arbitrary environment spectral density.

3.2 Transverse white noise

If noise is transverse to the motion, $\mathbf{n} \equiv \mathbf{x}$, the Lindblad operator Eq.(12) is again reducible, the eigenvalues being

$$\begin{aligned} z_{0,1} &= -\tfrac{\Gamma}{2} \pm \tfrac{1}{2}\sqrt{\Gamma^2 - (2vq)^2} \\ z_{2,3} &= -\tfrac{\Gamma}{2} \pm \tfrac{1}{2}\sqrt{\Gamma^2 - (4vQ)^2} \end{aligned} \tag{15}$$

where $z_{0,1}$ enter the SS dynamics and $z_{0,1}$ determine ZB. The common feature of both pairs is that for increasing Γ they exhibit a crossover from an "underdamped" (secular) regime, where $\Im z_i \neq 0$, to an "overdamped" (non secular) regime where eigenvalues are real and negative (see Fig.2). Notice that for large Γ two of the four real eigenvalues vanish as $z \propto v^2/\Gamma$, and the corresponding dynamics is "frozen". This is a manifestation of the Zeno effect determined by the continuous quantum measurement of the particle by the noisy field.

The fact that sectors such that $\hat{\zeta}^{(\mathbf{K},\mathbf{K'})}$ has Zeno-like eigenvalues exist, means that there may be overdamped modes of the wave-packet motion The consequences are apparent in the behavior of SS, shown in Fig. 3,

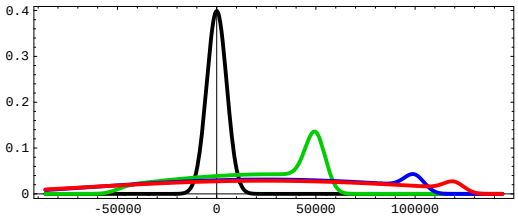

Figure 3. Marginal probability density $\varrho_{\mathbf{x}}(x,t)$ for a 1D-wavepacket of well defined chirality. Here y is expressed in units of the lattice distance a and per $t = 0, 5, 10, 12$ in units of $10^4\, a/v$. For $\Gamma/\Delta = 0.5$ (upper panel) the coherent peak and the incoherent tail are shown. For $\Gamma/\Delta = 2$ (lower panel) the incoherent peak is frozen close to the origin (notice the different spatial scale of the two figures).

where we consider a gaussian wave-packet with initial width Δ in the distribution of K_x. Spin-resolved marginal probability densities are given by the simplified expression

$$\varrho^{\sigma}_{\mathbf{x}}(y,t) = \int \frac{dq}{2\pi} \mathrm{e}^{-\frac{q^2}{8\Delta^2}}\, \chi_{\sigma\sigma}(q,t)\, \mathrm{e}^{iqy} \qquad (16)$$

where the variable Q has been integrated out. Modes corresponding to $q < \Gamma/(2v)$ are overdamped, therefore we expect a strong noise regime ($\Delta < \Gamma/v$) where all modes are overdamped, whereas only part of them are in the weak noise regime ($\Delta > \Gamma/v$).

The dynamics of a wave-packet prepared in an eigenstate of chirality is illustrated in Fig. 3. In the weak noise regime (upper panel) wave-packets show a coherent component moving with constant velocity ($\pm v$) which disappears in a time $t \sim 1/\Gamma$. They leave behind an inelastic tail, due to the presence of overdamped modes. For larger Γ the inelastic processes prevail, all the modes are overdamped (Fig. 3, lower panel) and the peak represents an incoherent mixture of both chirality eigenstates. Wave-packets prepared in a superposition of eigenstates of the chirality are shown if Fig. 4 at a fixed time. In the weak noise regime they show SS, the two separated coherent peaks keeping their initial width, independently of Γ. For strong noise spin-separation is suppressed and the wave-packet shows a single incoherent peak "frozen" at the initial position.

ZB oscillations are derived starting from the eigenvectors corresponding to the second pair of eigenvalues Eq.(15). In particular the ZB part of the position operator Eq.(7) is given, for a gaussian wave-packet and suitable initial conditions, by the simple form

$$\langle y_{ZB}(t)\rangle = \mathrm{e}^{-\frac{\Gamma}{2}t} \int \frac{dK}{2K} \frac{\mathrm{e}^{-\frac{K^2}{2\Delta^2}}}{\sqrt{2\pi}\Delta} \frac{z_3 \mathrm{e}^{i\omega t} - z_2 \mathrm{e}^{-i\omega t}}{z_3 - z_2}$$

where $\omega = \sqrt{\Gamma^2 - (4vK)^2}$ (Fig. 5). In the weak damping regime $\Gamma < 4vQ$, oscillation disappear only

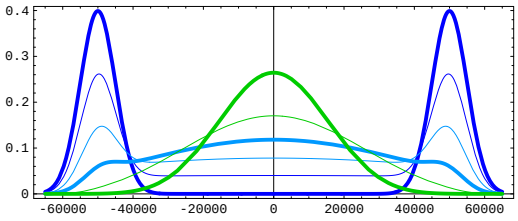

Figure 4. Marginal probability density $\varrho_{\mathbf{x}}(x,t)$ for $t = 5 \cdot 10^4\, a/v$, for a superposition of chirality states. Curves for $\Gamma/\Delta = 0, 0.2, 0.5, 1$ (blue) show SS. For $\Gamma/\Delta = 2, 5$ (green) SS is suppressed.

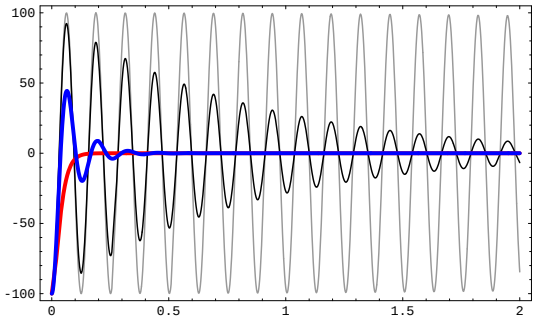

Figure 5. ZB component of the average position $\langle y(t)\rangle_{ZB}$ vs. time ($10^4\, a/v$ units) for transverse white noise. Here a superpositon of chirality states with dispersion $\Delta = 10^{-4}/a$ about $K_0 = 50\Delta$. Weak noise $\Gamma < \Delta$ has no effetto on the signal (grey curve) whereas for larger values $\Gamma/(4vK_0) = 0.025, 0.25, 1$ $\langle y(t)\rangle_{ZB}$ decays exponentially (black) and eventually reaches the overdamped regime (red).

for times $t > 2/\Gamma$, more slowly than for longitudinal noise. Instead small values of $|Q|$ determine overdamped modes in ZB.

We notice that the qualitative effect on SS and ZB of transverse and longitudinal noise is reversed: the former determines strong SS suppression, while the latter produces stronger dephasing of ZB oscillations. This is a consequence of the anisotropic coupling of noise in $\delta\mathcal{H}$, Eq.(3). It is related to the conservation of σ_z and it is reminiscent to the properties of certain nanodevices for quantum computation of exhibiting optimal operating points. On this basis we may argue that the same conclusions hold for general spectral density $J_P(\omega)$ of the environment.

Finally, since ZB oscillations are overdamped only if $\Gamma > 2v|Q|$, in the opposite regime $2v|Q| \gg \Gamma \sim \Delta$ noise will affect mainly SS. In these conditions weakly damped ZB oscillations may coexist with overdamped SS, or at least with a substantial incoherent tail of the wave-packet. This conclusion depends on the low-frequency behavior of the spectral density, holding for instance in the ohmic case $J_P(\omega) \sim \omega$.

4 Further remarks and conclusions

We have discussed the dynamics of one-dimensional wave-packets in the presence of noise, however many

qualitative conclusions can be extended to an arbitrary wave-packet with any finite spread $\Delta_{\mathbf{n}}$ of $K_{\mathbf{n}}$. For instance, since small values of q, corresponding to overdamped modes (except for longitudinal noise), are always present, SS will show an incoherent tail.

An appealing property of ZB in graphene is that, contrary to the case of electron-positron superpositions, ZB oscillations of the wave-packet extend over a mesoscopic distance. For $\langle Q\rangle \gg \Delta$ the amplitude of $\langle \mathbf{r}(t)\rangle_{ZB}$ scales as $\sim 1/\langle Q\rangle$. Although it is suppressed for wave-packets centered in the vicinity of the Dirac points, $\langle Q\rangle \ll \Delta$, for suitable values of $\langle Q\rangle$ it may be several hundreds of lattice spacings a large. This is encouraging for possible experiments aiming at observing ZB in graphene. Our results suggest that this is still true for wave-packets with $\langle Q\rangle \ll \min[\Delta, \Gamma/(4v)]$, even in the presence of an incoherent tail.

A general feature of the problem is expressed by the transformation Eq.(5). It shows that the pseudo-spin dynamics is very sensitive to low-frequency fluctuations of the environment.

We finally remark that our model shows that the effect of noise on the dynamics of QP's is completely described by the effect on the dynamics of the pseudo-spin. This is also true for controls operated by electromagnetic fields. This fact may be used for studying quantum control of photocurrents in chiral many body system. In this perspective it is worth stressing that effective control of the pseudo-spin dynamics by electromagnetic fields also opens ports to noise, which will have strongly anisotropic effects on the QP's motion.

References

A.O. Caldeira and A.J. Leggett, (1981) Influence of Dissipation on Quantum Tunneling in Macroscopic Systems *Phys. Rev. Lett.* **46** 211-214.

A.H. Castro Neto, F. Guinea, N.M.R. Peres, K.S. Novoselov and A.K. Geim, (2009) The electronic properties of graphene, *Rev. Mod. Phys.* **81** 109-162.

G. Chen *et al.*, *Quantum computing devices*, Chapman & Hall/CRC, 2007

C. Cohen-Tannoudji, J. Dupont-Roc, G. Grynberg, *Atom-Photon interaction: Basic processes and application*, Wiley Science Paperback Series, 1992; M.O. Scully and M.S. Zubairy, Quantum Optics, Cambridge Univ. Press, Cambridge, 1997.

J. Cserti ang G. David, (2006) Unified description of Zitterbewegung for spintronic, graphene, and superconducting systems *Phys. Rev. B* **74** pp. 172305-1-4.

G. Falci et al. (2009), Dynamics of Weyl wavepackets in a noisy environment *Physica E*

G. Falci and R. Fazio, Quantum computation with Josephson qubits, in *Quantum Computer, Algorithms and Chaos*, edited by G. Casati, D. L. Shepelyanskym P. Zoller and G. Benenti, IOS Bologna, 2005, and references therein;

W. Greiner, *Relativistic quantum mechanics*, Springer, 2003.

.P. Gusynin, S.G. Sharapov, and J. P. Carbotte, (2007) AC conductivity of graphene: from tight-binding model to 2+1-dimensional quantum electrodynamics *arXiv:0706.3016*.

V. Hakim and V. Ambegaokar, (1985) Quantum theory of a free particle interacting with a linearly dissipative environment *Phys. Rev. A* **32** 423-434.

M. I. Katsnelson, K. S. Novoselov, (2006) Chiral tunnelling and the Klein paradox in graphene
A. K. Geim, *Nature Physics* **2**, pp. 620-625.

. Mangano, J. Siewert and G. Falci, (2008) Sensitivity to parameters of STIRAP in a Cooper Pair Box
Eur. Phys. Journ.-ST 160 259-268.

E.J. Mele, P. Kral, and D. Tomanek, (2000) Coherent control of photocurrents in graphene and carbon nanotubes *Phys. Rev. B* **61** 7669-7677.

K.S. Novoselov *et al.*, (2004) Electric field effect in atomically thin carbon films *Science* **306** 666-669.

K. S. Novoselov, A. K. Geim, S. V. Morozov, D. Jiang, M. I. Katsnelson, I. V. Grigorieva, S. V. Dubonos, A. A. Firsov, (2005), Two dimensional gas of massless Dirac fermion in graphene *Nature* **438** 197-200.

E. Paladino, L. Faoro, G. Falci, and R. Fazio, (2002) Decoherence and 1/f Noise in Josephson Qubits *Phys. Rev. Lett.* **88** 228304-1-4;

F. Plastina and G. Falci,(2003) Communicating Josephson qubits *Phys. Rev. B* **67** (2003) 224514-1-4.

. Siewert, T Brandes and G. Falci, (2009) Advanced control with a Cooper-pair box: Stimulated Raman adiabatic passage and Fock-state generation in a nanomechanical resonator *Phys. Rev. B* **79** 024504-1-6;

G.W. Semenoff, (1984) Condensed-Matter Simulation of a Three-Dimensional Anomaly *Phys. Rev. Lett.* **53** 2449-2452.

A. Wallraff *et al.*, (2004) Circuit Quantum Electrodynamics: Coherent Coupling of a Single Photon to a Cooper Pair Box,
Nature **431**, 162-169.

U. Weiss, *Quantum dissipative system*, Word Scientific.

J.Y. Vaishnav, C.W. Clark, (2008) Observing Zitterbewegung with Ultracold Atoms *Phys. Rev. Lett.* **100** 153002-1-4.